Geophys. J. R. astr. Soc. (1984) 79, 635–649

Electrical resistivity structure of the Senegal basin as determined from magnetotelluric and differential geomagnetic soundings

M. Ritz *Office de la Recherche Scientifique et Technique Outre-Mer, B.P. 1386, Dakar, Sénégal, West Africa*

Received 1984 May 8; in original form 1983 July 11

Summary. The methods of magnetotelluric (MT) and differential geomagnetic soundings (DGS) have been applied to study the electromagnetic response of the structure of the Senegal sedimentary basin. The measurements at 10 sites were carried out along a profile running perpendicularly across a zone of north–south flexures and faults over the period range 10–1000 s. Variation of periods up to 10 000 s were obtained at two sites. The anomalous geomagnetic variation field across the major fault zone is characterized by an increase in the magnetic eastward component. Two-dimensional modelling of the apparent resistivities and phases reveals a highly anomalous upper crustal structure involving a low-resistivity zone in the central part of the basin (less than 30 Ωm). To satisfy the additional long-period data at two sites, a deep conductor is also required at a depth below 300 km with a resistivity less than 10 Ωm. The crustal discontinuity located ~ 200 km off the coast is possibly related to the opening of the Atlantic Ocean. The difficulty in resolving the question of the nature of the crust in this region results in part from the limitations of the methods used at present for this determination.

1 Introduction

During the last 3 yr, the time-varying electric and magnetic fields have been measured by the Office de la Recherche Scientifique et Technique Outre-Mer (ORSTOM) at 10 sites along a profile crossing the Senegal basin and extending along the 14th parallel. A schematic cross-section of the sedimentary basin as redrawn from De Spengler, Castelain & Leroy (1966) and Liger (1980) shows the general pattern of the area from the Atlantic coast to the Mauritanides along the latitude of the Dakar Peninsula (Fig. 1). That cross-section shows a Precambrian crystalline basement dipping to the west under a wedge of post-Palaeozoic sedimentary rocks of more than 5 km (Mesozoic and Cenozoic sediments). The motivation for the field experiment was to determine the resistivity values associated with the zone of N–S flexures and faults along longitude 15°W and to see if changes in electrical character of the crust and/or upper mantle can be expected to occur between the deep basin and the zone outside of the actual post-Jurassic sedimentary basin. The present paper reports on

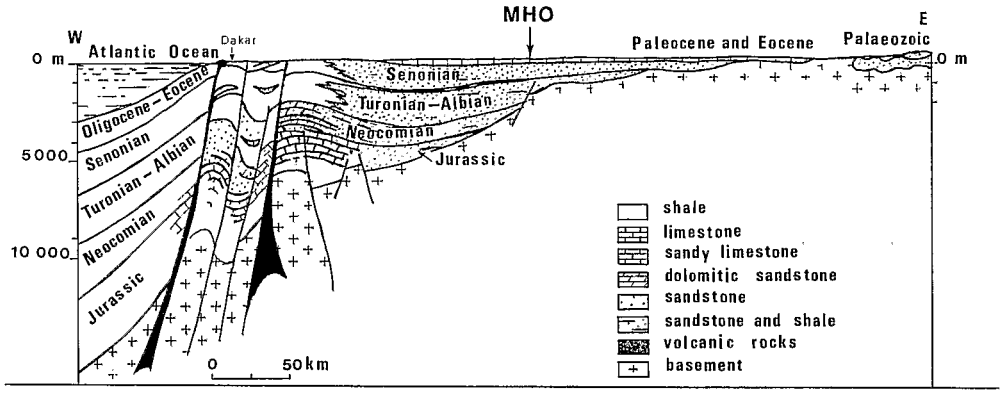

Figure 1. Cross-section of the Senegal basin from De Spengler *et al.* (1966) and Liger (1980).

the MT and DGS results from sites referred to in Table 1. The locations of the recording sites of this study are shown in Fig. 2. The full names, abbreviated station names as used in Fig. 2 and the station coordinates are given in Table 1.

The Senegal coastal basin situated on the western edge of Western Africa broadly extends to the boundaries of Senegal as it lies between the 10 and 21° northern parallels (Guinea Bissau and Mauritania). It is bounded in the east by the West African mobile belt (Hercynian orogenic belt–Mauritanides). This basin was formed during the Jurassic period before the transgression of the Cretaceous period, then extended to the Tertiary with a great subsidence towards the west (Dillon & Sougy 1974). During this period, between 210 and 170 Myr, at the end of the different stages of rifting of the Trias, one witnesses the aperture of the Atlantic Ocean with the formation of a new oceanic crust (Le Pichon & Fox 1971). The subsidence and the Mesozoic rifting of the West African margin responsible for the formation of the Senegal basin was very likely accompanied by the intrusion of magmatic material into predominantly coast-parallel fissures and fractures (Van der Linden 1981).

Geophysical studies have been carried out in Senegal basin: gravity studies, electrical soundings, drillings and aeromagnetic profiles. The area between KAH and MBM showing a strong gravity gradient is interpreted in terms of thick mafic intrusions within the basement

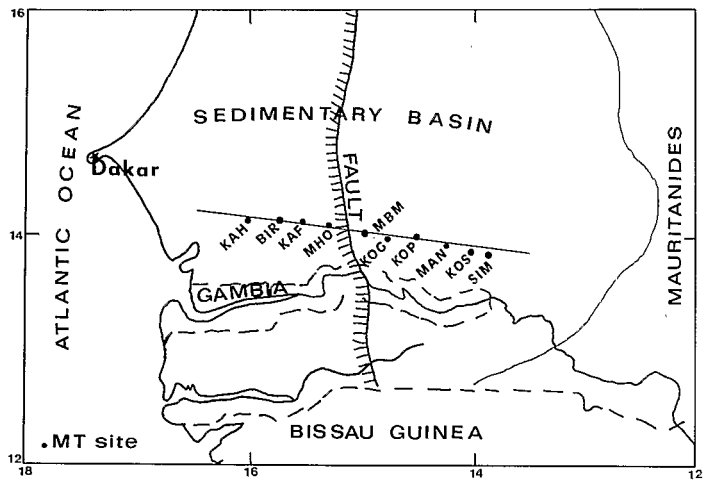

Figure 2. Location map of the magnetotelluric sounding sites in relation to the major fault.

Table 1. Mt sites, code names and geographic coordinates.

Station name	Code	Long. (W)	Lat. (N)
Kahone	KAH	16° 02′	14° 09′
Birkelane	BIR	15° 45′	14° 08′
Kaffrine	KAF	15° 33′	14° 06′
Malème Hodar	MHO	14° 18′	13° 56′
Mbaye Mbaye	MBM	15° 00′	14° 00′
Koungheul	KOG	14° 58′	13° 59′
Koumpentoum	KOP	14° 33′	13° 59′
Malème Niani	MAN	14° 18′	13° 56′
Koussanar	KOS	14° 03′	13° 52′
Sinthiou Malème	SIM	13° 55′	13° 50′

complex (Liger 1980). Many electrical soundings carried out with line AB of 6000 m give us an idea of the thickness of the sedimentary series above the basement (Compagnie Générale de Géophysique 1957). However, the depth of the investigation through the electrical soundings is relatively weak (of the order of 1000 m) and the resistant basement easily visible to the east, disappeared in the west from the meridian 15 °W. Below the deep basin, the nature and depth of the basement are generally unknown.

2 Observations and processing

Magnetic variations were measured using Mosnier sensors which give the H and D components of the magnetic field (Mosnier & Yvetot 1972). These are horizontal variometers with suspended magnet and feedback. The sensitivity is 10 mV γ^{-1}. Telluric variations trending N–S and E–W were detected through the measurement of the potential difference between pairs of lead electrodes situated 500 m apart and at a depth of 1.50 m. Magnetic and telluric signals were filtered and amplified in the period band ranging from 10 to 1000 s before reaching the recording equipment, which is composed of two 'Sefram' graphic recorders. The same equipment is found at the moving station and at the reference station. Recordings were made simultaneously at a reference station (SIM). The electromagnetic fields were recorded for one week at each site. Approximately one month of long-period MT data was recorded simultaneously at the two sites SIM and MHO. The analogue traces were digitized at 3 s intervals, by means of a trace-follower digitizing table.

Two methods have been used to study the structure basin:

(a) *Magnetotellurics*: the horizontal and orthogonal components of the electric and magnetic fields, which are measured at the surface, are combined by a complex transfer function, the impedance tensor Z. The elements of Z depend on the resistivity distribution and the orientation of the measuring coordinate system (Cantwell 1960; Madden & Nelson 1964; Vozoff 1972; Beblo & Björnsson 1978). Two parameters, the apparent resistivity $\rho_a(T)$ and the phase difference between the electric and magnetic field $\phi(T)$ are calculated as functions of period from the impedance tensor. For a two-dimensional earth (2-D), the principal impedance values are calculated with axes parallel and perpendicular to the strike of the 2-D structure (TE and TM directions). From these are derived the parallel and perpendicular resistivities and phases (Thayer 1975). For each period, the angular rotation of the impedance tensor yields an estimate of the structural strike. For each site, apparent resistivities and phases in the principal directions are computed and are plotted in Figs 3, 4 and 5.

(b) *Differential geomagnetic soundings*: the geomagnetic variation field produced by lateral variations in the telluric current system has a vertical component and produces

anomalous variations in the regional horizontal field. The total geomagnetic variations field is thus composed of a source component and an induced component produced by the telluric current system. Consequently, to study the variation field, a reference site is located so that it can be assumed to be influenced only by the regionally uniform telluric current system and by the source field, which is assumed to be uniform over the study area. By subtracting the horizontal field observed at this base station from the fields observed at the field stations, the anomalous field due to the non-uniform component of the telluric current can be determined (Babour & Mosnier 1977). Telluric current concentrations are controlled by the electrical conductivity structure of the crust and upper mantle. Under the assumption of a uniform source with infinite spatial wavelengths, the observed field field variations, comprised of normal and anomalous field variations, can be fitted statistically to the frequency-domain relation (Schmucker 1970):

$$\begin{pmatrix} H_a \\ D_a \end{pmatrix} = \begin{pmatrix} h_H & h_D \\ d_H & d_D \end{pmatrix} \begin{pmatrix} H_n \\ D_n \end{pmatrix} + \begin{pmatrix} \delta_H \\ \delta_D \end{pmatrix}$$

(H_a, D_a) is the Fourier transform of the anomalous field, i.e. the field associated with the lateral conductivity inhomogeneities, (H_n, D_n) denotes the Fourier transform of the normal field, and (δ_H, δ_D) is a residual field.

Geomagnetic field variations at Sinthiou Maleme (SIM) were chosen as the reference in calculations of the anomalous geomagnetic variation field across the basin. Site SIM is about 200 km east of the major fault (Fig. 2). At each station the azimuth θ of a linearly polarized, horizontal reference field that maximizes the correlated part of the anomalous field, is calculated. This direction is the preferential induction direction (Vasseur *et al.* 1977). In order to know the frequency dependence of the anomaly, we have computed the transfer function $G(f)$ linking the anomalous field at each site, to the normal field (SIM) projected on the induction direction. The response will be a maximum (or minimum) along this axis (Banks & Ottey 1974).

3 Results

3.1 MAGNETOTELLURIC RESULTS

We have calculated 10 tensor MT soundings covering the period range from 10 to 1000 s. The resulting principal axis orientation proved to be quite stable across the entire period band and the average principal direction is given in Table 2 for each station. We note a sudden change in the principal axis orientation between sites KOG and KOP. The axes are oriented N–S in the deep basin and at both MBM and KOG (this direction is roughly parallel to the strike of the prominent N–S trending fault), but are more E–W for all other sites (except KOS). It can be seen (Fig. 1) that the significant rotation occurs outside of the actual post-jurassic sedimentary basin and it is probable that this indicates the presence of boundaries between two structures of different electrical conductivity, mainly near the surface, but also at greater depths (Ritz 1983). Figs 3 and 4 show the calculated values for the apparent resistivities and phases from rotated impedance for all the 10 sites, separately for the TE and TM directions. The values of resistivities at the site KOP are elevated by a factor of 2 compared to the adjacent site KOG. At site KAF, which is about 40 km west

Table 2. Orientation of the principal axes of the impedance tensors (clockwise from north).

Station	KAH	BIR	KAF	MHO	MBM	KOG	KOP	MAN	KOS	SIM
Orientation	33°	13°	13°	7°	16°5	17°	48°	66°	Undefined	62°

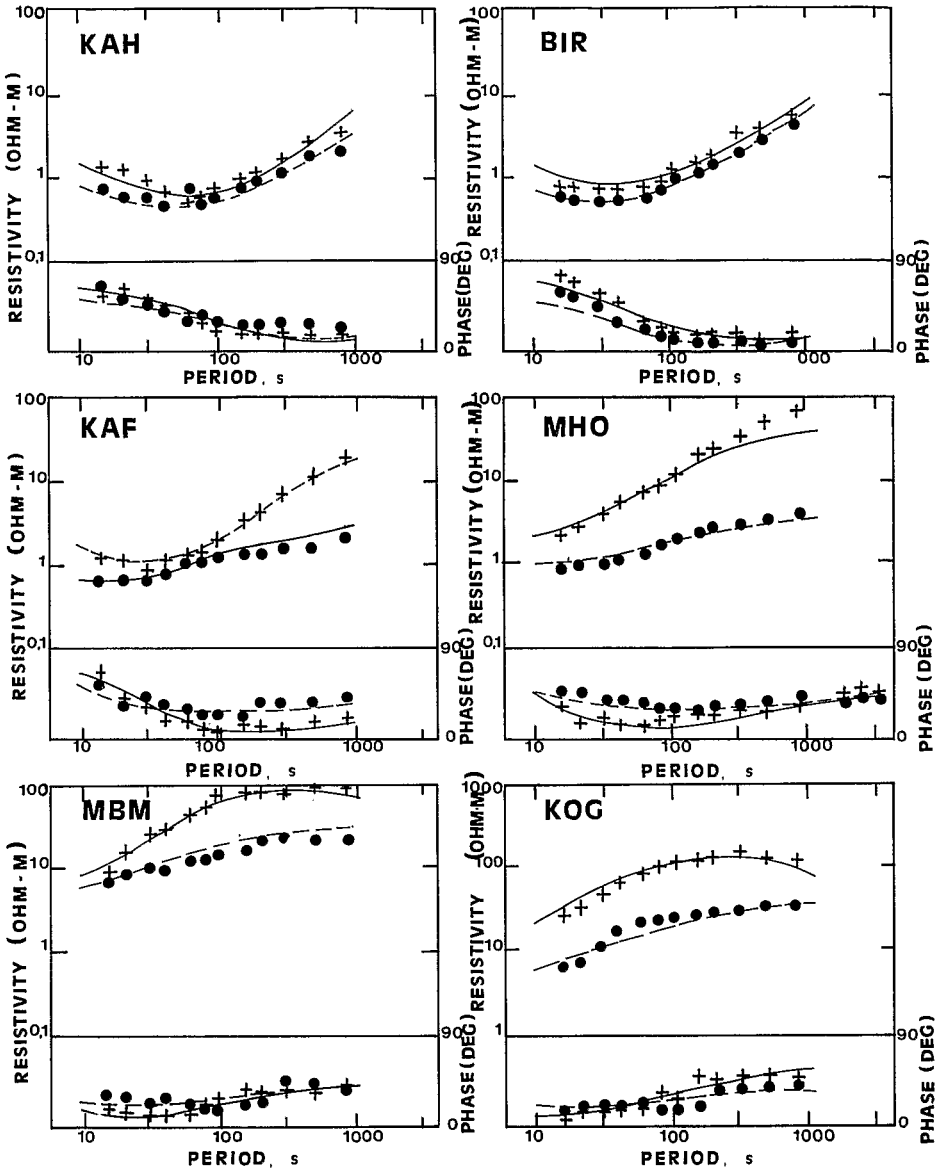

Figure 3. Apparent resistivities and phases for the MT sites on the Senegal basin. The principal resistivities and phases for the TE and TM directions are shown by crosses and solid circles, respectively. Solid and dashed lines through the measured values are theoretical curves calculated from the model shown in Fig. 10.

of the fault, the significant divergence of the TE and TM amplitudes at periods above 100 s shows clearly the effect of lateral resistivity variations. This type of behaviour continues in a progressively increased manner, from west to east, up to the site KOG (about 30 km east of the fault). The long-period MT data at the two sites MHO and SIM, until about 10 000 s, are presented in Fig. 5. The long-period data for site MHO display increasing anisotropy with increasing period. The azimuths of the maximum resistivity principal direction are nearly invariant over all the period bands analysed.

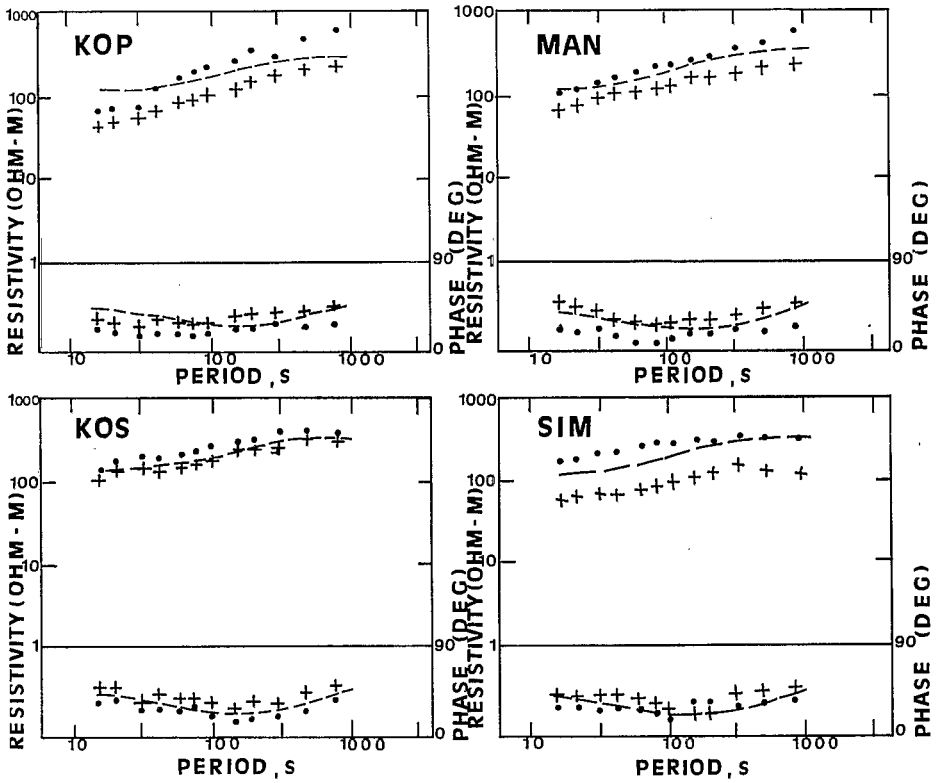

Figure 4 – *continued.*

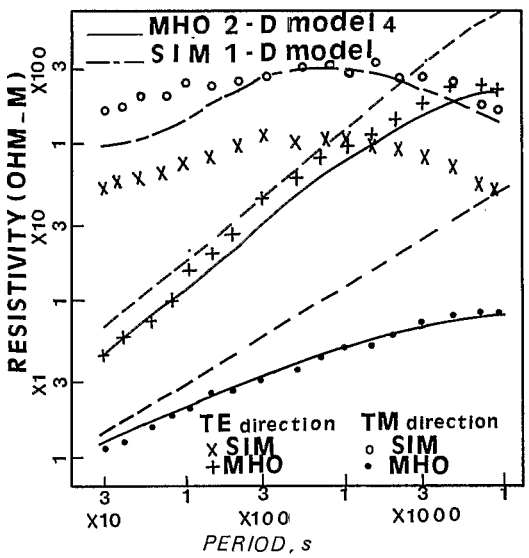

Figure 5. TE and TM sounding curves at the long-period MT sites. Solid and dashed curves are the result of the 2-D model calculations at MHO with upper crustal conductor present (model 4) and removed (model 1), respectively. The curve defined by the long and short dashes is the response of the 1-D model shown in Fig. 10 at SIM.

For the region to the east of KOG, the data for site KOS are the most nearly 1-D, as can be seen from the near coincidence of the major and minor apparent resistivities. The data for sites KOP, MAN and SIM show splits between the TE and TM amplitudes, but the phase data practically coincide (except MAN). Through site SIM, difference between resistivity values for the two directions, is relatively constant throughout the period range (Fig. 5). In this region, with a thin sedimentary cover (Fig. 1), there are possibly some 2- or 3-D features maintaining the separation in the data. Theoretical calculations show that local 2- or 3-D surface inhomogeneities have a strong influence on the amplitude data and but a weak influence on the phase data. In this situation the major curve (TE or TM) will be closer to the 1-D curve without shallow heterogeneity (Berdichevsky & Dimitriev 1976). The maximum apparent resistivity observations through sites KOP, MAN, and SIM are practically identical with the observations at site KOS (Fig. 4), where data are not distorted

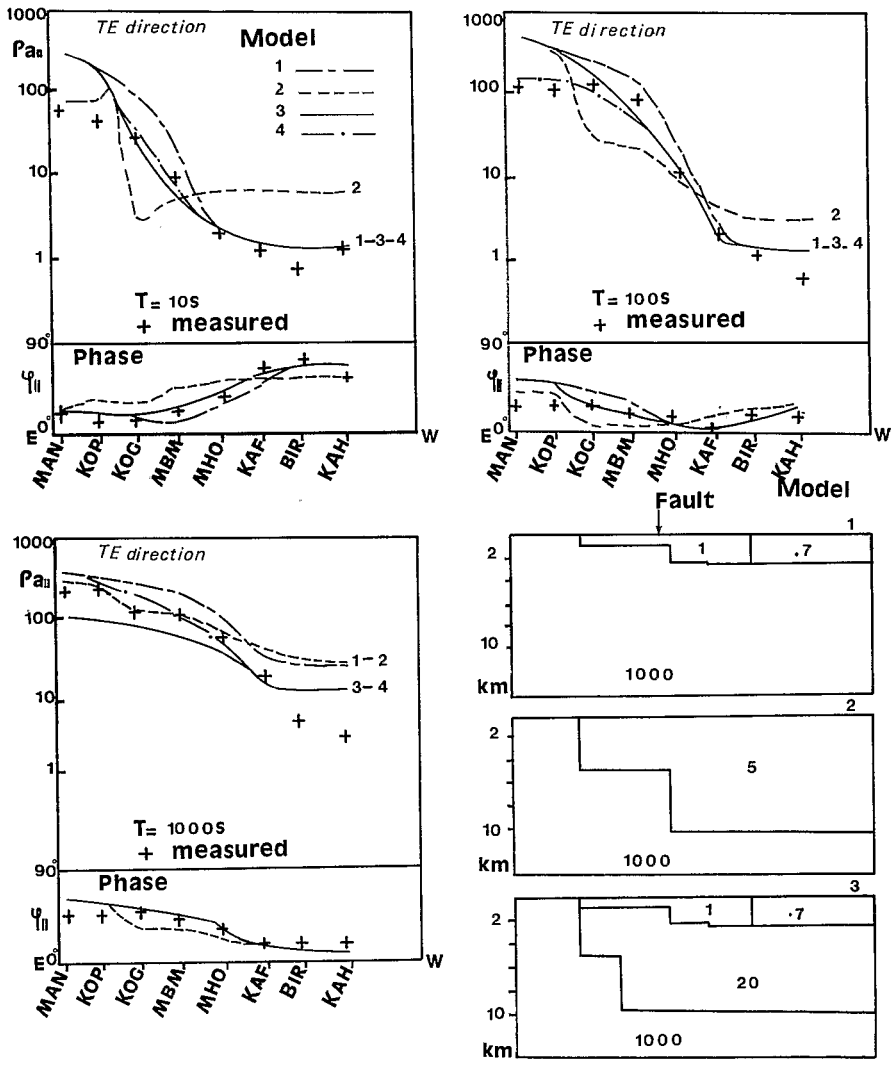

Figure 6. Variation of MT data along the profile for the TE direction case, for periods 10, 100 and 1000 s and results of calculation for three models shown at the right side of the figure. (The overburden is not displayed in these models.) At 1000 s, the phase curves are similar for the models 1 and 3.

significantly by the presence of the lateral near-surface inhomogeneities. This obvious similarity therefore point to a similar 1-D conductivity structure under these four stations. The apparent anisotropy at KOP, MAN and SIM indicates distortion of the electromagnetic field due to lateral heterogeneities which are shallower than the penetration depth of the shortest period measured.

Electromagnetic fields penetrate into the Earth to depths which vary depending on the Earth conductivity and the period of the signals. The depth of sounding can be related to period by use of the concept of the penetration depth $[p(\mathrm{km}) = \sqrt{10\,\rho T}/2\pi$, ρ is the resistivity in ohm metres, T is the period in seconds]. The sedimentary layers of the Senegal deep basin were expected to have low resistivity. Over a 1 Ωm basin, we measured the resistivity from the surface to a depth of about 1500 m at 10 s, 5000 m at 100 s and to about 16 km at 1000 s. Figs 6 and 7 show the observed values of the TE and TM apparent resistivities and phases along the profile between MAN and KAH for 10, 100 and 1000 s. The TE resistivities form a gradual transition between the high resistivity (towards the east) to low resistivity region (towards the west). The apparent resistivity along the profile, for the sites to the west of KOG, rises somewhat with the penetration depth indicating layers.

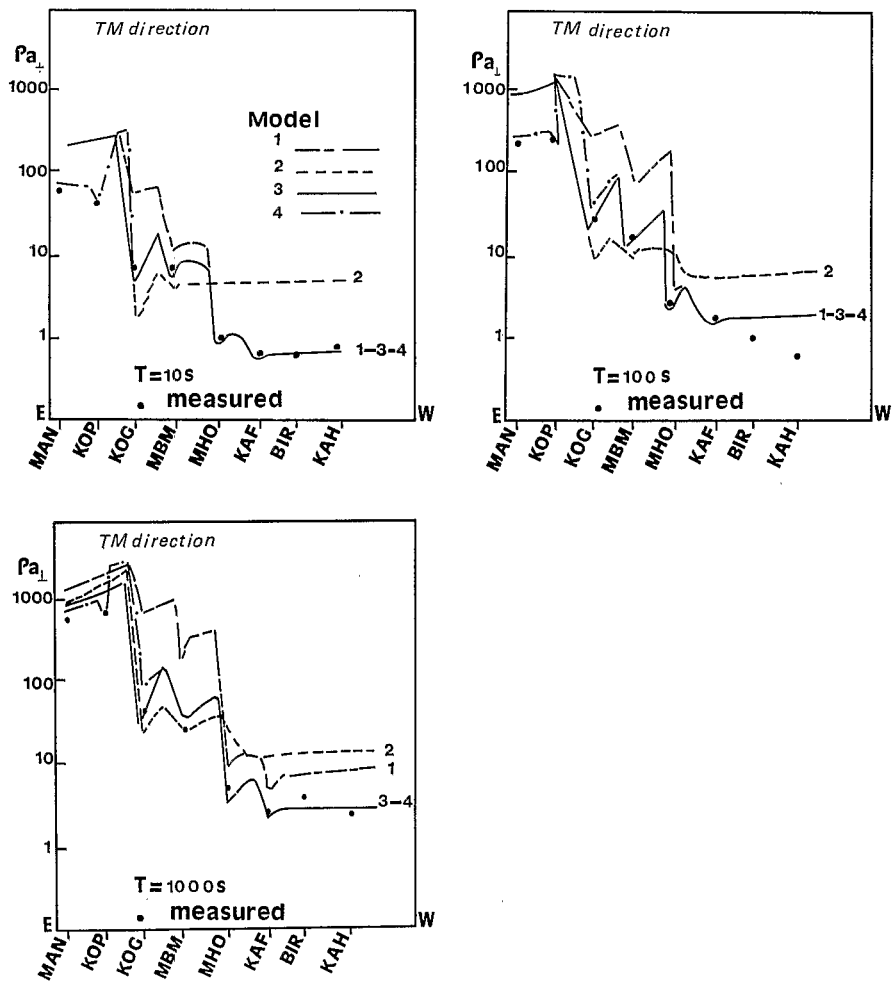

Figure 7. As Fig. 6 for the TM direction (apparent resistivities only).

When the period increases at site MHO from 10 to 100 s ($p \sim 1.5-6$ km), both TE and TM apparent resistivities increase, indicating penetration of the electromagnetic fields into a resistive layer. The variation in apparent resistivity is insignificant for KAF, BIR and KAH, reflecting lateral homogeneity of the surface sediments within the vicinity of these sites. No detailed knowledge of the deep basin is available; however, the basement slopes down from about 800 m in the east (KOS) to about 10 km in the Dakar area (Fig. 1). The top of the basement is a layer boundary at which the resistivity is increased by a factor between 10 and 1000 (Losecke, Knödel & Müller 1979). It seems reasonable to assume that the resistive layer under MHO could be associated with the basement at depths between 1.5 and 6 km, and that the horizon of the layer continuously deepens towards KAF, BIR and KAH (at some depth greater than 6 km). In the case of TM direction, on the western border of the profile, Figs 6 and 7 show steep resistivity gradients as the basement front is approached. Apparent resistivities of several hundred ohm metres are associated with the crystalline or metamorphic basement.

3.2 MAGNETIC RESULTS

The amplitude of the magnetic eastward geomagnetic variation field (D component) increases for KOG, MBM, MHO, KAF, BIR and KAH, with the result that the amplitude of the D component at MHO is about twice that of the reference station SIM. The variations in the horizontal north (H) component appear to be identical at the 10 stations. We have calculated the induction direction for these sites. These directions lie between 90° and 110° in the period range from 30 to 1000 s. Fig. 8 shows the frequency dependence of the induction direction at a representative site (KAF). The residual geomagnetic variation field D_a is linked only to the horizontal east (D_n) component. We have calculated the transfer function $G(f)$ and the phase linking D_a, obtained at each site, to the normal field (SIM), projected on the induction direction 100°. The modulus of the maximum response and the phase of $G(f)$ as a function of the period are presented for the site KAF in Fig. 8. The anomalous geomagnetic variation field along the profile with the period of 100 s is displayed in Fig. 9. The anomalous field D_a/D_n has a maximum between MHO and KAF at 100 s. The anomalous geomagnetic field variation across the fault could be accounted for by one or more of the following: concentration of currents by conductive structures (sediments), direct induction in the underlying structures so that the 2-D modelling could

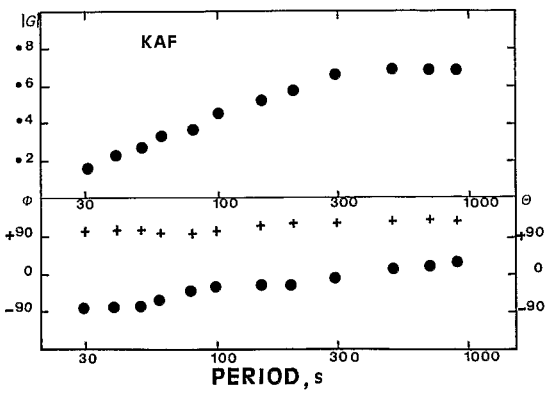

Figure 8. Transfer function G as a function of period (modulus and phase) computed between the anomalous geomagnetic variation field D_a (KAF) and the normal horizontal field (SIM) projected on the induction direction θ (crosses indicate the induction direction).

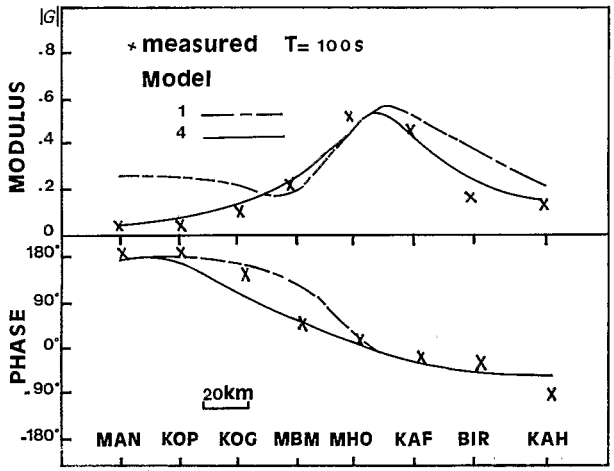

Figure 9. Observed anomalous horizontal field along the profile with a period of 100 s. The lines through the measured values are theoretical curves calculated from models presented in Fig. 6. Model 4 not represented in Fig. 6 (*cf.* p. 645).

be used to fit the observed anomaly (Bailey *et al.* 1974; Gough 1981; Gregori & Lanzerotti 1982). Whatever the inductive mechanism, a maximum depth for the current system can be made from the well-defined anomaly of the Fig. 9 (Gough 1973). Estimate gives a maximum depth of 25 km. In differential geomagnetic sounding basins with well conducting sediments can be recognized by large disturbances of the normal geomagnetic field. This is due to telluric currents, which are induced in the conductive sediments of the basin in addition to the large-scale uniform telluric current system in the area. As the additional electric current system in the basin flows only in the striking direction of the basin (that is about N–S for the Senegal basin), the anomalous geomagnetic variation field is only measured in the *D* component of the magnetic variations. The *H* component is not affected by the non-uniform component of the telluric current system (Babour & Mosnier 1979). The Senegal basin consists of two parts along the profile, an eastern thin part and a western thicker part (Fig. 1). At a first glance, it appears that electric current flow in the sediments of the deep basin might cause this anomalous horizontal field.

4 Modelling

On the basis of the above observations, modelling for the 10 sites was done by using a combination of inverse 1-D computations (Jupp & Vozoff 1975), and 2-D forward modelling (Stodt 1978). In constructing the 1- or 2-D models in order to fit the electromagnetic data the following assumptions were made.

(1) In the region at some distance of the fault, about 60 km east and more, the resistivity is a function of depth only (similarity of the major and minor apparent resistivity at KOS).

(2) The electrical conductivity structure beneath a part of the basin is 2-D, so that a line from KOG to KAH direct would be at right angle to the N–S trending fault.

(3) An overburden of average resistivity 15 Ωm extends down to 800 m, overlaid the region. This assumption is supported by the electrical soundings for the uppermost sedimentary layer and corresponds to the known structure of the basin.

(4) The zone of N–S flexures and faults along longitude 15 °W marks the line of division between two contrasting regions. This is based on the sudden decrease of the apparent resistivity between KOG and MHO at 10 s (Figs 6 and 7).

The inversion was done on both the major apparent resistivity and phase data simultaneously for stations east of the site KOG. A layered earth model of four layers is adequate to describe the major data (Fig. 4). For SIM, there is improvement of fit at periods greater than 1000 s if the number of layers is increased to one (Fig. 5). This model indicates a resistive crust underlain by material of 50 Ωm starting at a depth of about 20 km (Fig. 10). For site SIM, the model was developed to estimate the highly conducting portion of the mantle. A five-layered model suggests a conducting layer of approximately 10 Ωm beginning at 300 km.

At the right side of Fig. 6 three of the several 2-D models constructed are shown as a simple approximation to the resistivity distribution. The simplest model is the model 1 with a major lateral conductivity change between MBM and MHO: On the hand basement, on the other hand the deep basin extending to a depth of 1.5–3 km with $\rho = 1-0.7$ Ωm. Model 2 consists of well-conducting material with several kilometres thickness (until 10 km) beneath the deep basin. Model 3 is a combination of models 1 and 2 with various conductors added to the sedimentary basin at crustal depths. Model 4 (not displayed in Fig. 6) is similar to model 3 with a conductive crustal layer (~ 50 Ωm) at a depth between 20 and 30 km under

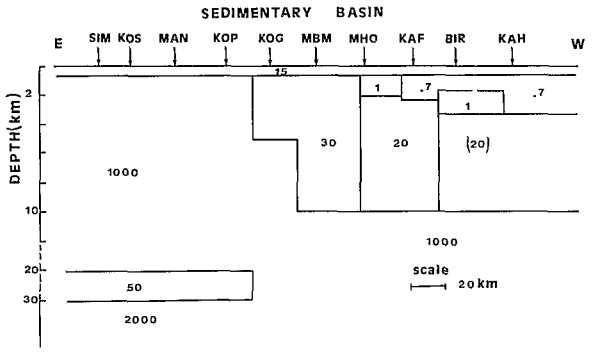

Figure 10. East–west 2-D resistivity model for Senegal basin. The conducting portion of the mantle beginning at 300 km is not represented. The numbers indicate assumed resistivities in ohm metres. The parameter in brackets is poorly resolved.

KOP and MAN. Observations and model calculations have been made with the periods, 10, 100 and 1000 s (Figs 6 and 7). The apparent resistivities are shown for both TE and TM direction cases, the phases are shown for the TE direction case only. The phases for model 4 are not illustrated here. For the TE and TM directions the results of measurements and the calculated curves fit best for model 4. However, between MHO and KAH at periods less than 100 s, the same apparent resistivity curves are obtained for the models 1 and 3. At 1000 s, the difference between these resistivity curves is relatively little, the periods of variations are not long enough to discriminate between a resistant layer (model 1) and a good conducting one (model 3). The distinction between these two models cannot be estimated accurately at this stage so that we are not convinced that an anomalously good conducting layer exists under the deep basin. Long-period MT data for site MHO and the results for models 1 and 4 are represented in Fig. 5 for the purpose of comparing the model resistivities with the measured resistivities. These model calculations for long-period variations have mainly been made to see if a well-conducting zone may be assumed below the deep basin. For periods of 1000 to 10 000 s, there is a significant difference in the form of the apparent resistivity curves (TE and TM directions) calculated for the models 1 and 4. It is interesting to note the increase in the discrepancy between the results of measurements and the

calculated curves for model 1. A resistant layer below the deep basin at MHO is inadequate to fit the TE and TM values at long periods. Two-dimensional modelling of the long-period data from this site shows that the class of models which fit the MHO observations suggests that there is an anomalously good conductive layer in the upper crust. Because of the lack of long-period MT data at BIR and KAH, the horizontal extension of the well-conducting layer can be reliably determined only to a distance of about 45 km to west of the major fault. On the basis of the model studies (Figs 5, 6 and 7), it seemed to be reasonable to assume the existence of a good conductor in the upper crust (< 10 km thick) to a distance of about 45 km to each side of the N–S trending fault.

Model 4, between KOG and KAF, was adapted to provide a reasonable fit for the MT data (Fig. 10). The results for final model are also shown in Figs 3 and 5 along with the field results (TE and TM directions). At long periods adjustment of the model can be achieved by placing the transition from high to low mantle resistivity at approximately 300 km at SIM and MHO.

For the geomagnetic data two simple 2-D models are used. They correspond to the models 1 and 4 (see Fig. 6). Model 4 is not presented in Fig. 6 (*cf.* p. 645). If we assume the models to strike in a N–S direction, we can compare the calculated data with the magnetic eastward component of the field measurements. The modulus and phase of D_a/D_n are plotted along the profile for 100 s in Fig. 9. Model 1 shows that electric current flow in the well-conducting sediments of the basin produces excessive anomalous horizontal fields at the westernmost sites.

The observed values of D_a/D_n along the profile best fit the model 4, where a crustal conductive structure is added to the sedimentary model. The response of this type of model across the basin is shown with the observed anomalous geomagnetic variation field in Fig. 9. The study of the anomalous geomagnetic variation field along the profile partly contributes to a more exact determination of the upper crustal layer under KAF, BIR and KAH and suggests that an anomalously well-conducting layer is quite likely below the deep basin.

Final adjustment of the model 4 was made to provide an adequate fit for the values of the TE and TM apparent resistivities and phases (Figs 3 and 4). Although the final model (Fig. 10) gives results which approximately correspond to the field results, the uniqueness of this model cannot be guaranteed because of the number of assumptions involved.

To summarize, the following can be said: the MT measurements can be interpreted in a satisfactory way only if an anomalously well-conducting layer is assumed below the sedimentary basin between KOG and KAF. This layer begins close to the surface beneath the eastern basin (KOG and MBM) and dips to the west under a wedge of Mesozoic and Cenozoic sediments of more than 2 km; it has a resistivity of about 20–30 Ωm, and a thickness of less than 10 km. Geomagnetic measurements suggest the lateral extension of this layer under BIR and KAH. It is interesting to note that the two methods are necessary to show the existence in this region of the upper crustal conductor. Crustal electrical resistivity structure in Senegal basin derived from MT and DGS measurements is shown in Fig. 10.

5 Discussion

5.1 NATURE OF THE CRUSTAL RESISTIVITY ANOMALIES

The zone of enhanced electrical conducting which has been inferred at lower crustal depths beneath the eastern basin is common. High conductivities for depths of about 15–35 km have been found by many investigators using the magnetotelluric, geomagnetic and controlled

source experiments below different tectonic provinces of the Earth (see, for example: Blohm, Worzyk & Scriba 1977; Van Zijl 1977; Jones & Hutton 1979; Connerney, Nekut & Kuckes 1980; Edwards, Bailey & Garland 1981; Ingham & Hutton 1982; Kurtz 1982). Regarding conducting zones in a depth of 15 km and more, several theories exist: partial melting in the presence of a small quantity of water of the moderate temperatures (Lebedev & Khitarov 1964), hydration processes (Hyndman & Hyndman 1968), a combination of basic rock type and high pore fluid pressures (Lee, Vine & Ross 1983). In this area no measurement of the heat flow has been obtained and higher than normal temperatures in the crust cannot be ruled out as a possible interpretation of the crustal conducting layer below the eastern basin. In order to determine the nature of the conducting layer in the crust, it is very desirable to couple electromagnetic methods with seismic investigations.

An important feature of the electromagnetic results is that the entire upper crust down to about 10 km has a resistivity less than 30 Ωm (in western basin, Fig. 10). The sedimentary unit represents the actual post-Jurassic basin with Cenozoic and Mesozoic sediments. Resistivity of this unit is of about 1 Ωm. In Canada, the Mesozoic–Cenozoic sediments of the Coastal Plain may have resistivities as low as a few ohm metres (Greenhouse & Bailey 1980). Beneath this sedimentary sequence the resistivity is anomalously low (20–30 Ωm). A range of possible interpretations for this zone is summarized here. Resistivities of 30 Ωm or less can be related to the presence of the thermal fluids (Thayer 1975). Electrolytic conduction in pore fluids is the dominant conduction mechanism in the upper 8 km and a shallow conductor at crustal depth can then be explained by increased porosity in the host rock, increased temperature, or increased salinity of the fluid. The conductor under the deep basin could be associated with saline water, slight variations in porosity could then provide resistivity variations as suggested by Fig. 10. The low resistive zone could be also in relations with the existence of a fractured zone with high water content along the zone of N–S faults. The difference between the low (20 Ωm) and the relatively low (30 Ωm) zone might arise from a difference in degree of fracture and degree of water content. This zone can be also connected with the presence of conducting minerals (Gough 1981).

5.2 TECTONIC IMPLICATIONS

The most significant result of the present experiment is the existence of a crustal discontinuity in the basin located ~200 km off the Atlantic. The tectonic history of the basin accounts perhaps for the present-day variations in electrical characteristics and depth of conductors located in the lower crust below the eastern basin and in the upper crust beneath the deep basin.

In the basin, the expected crustal thinning in the transition from continental crust in the east to an oceanic type crust in the Dakar area (Rabinowitz 1979; Liger 1980) makes it is difficult to say whether the good conductor below the deep basin marks an anomalous layer in the upper crust or the crust–mantle boundary. Liger (1980) interprets the coastal positive Bouguer gravity values in terms of a considerable thinning of crust and gives a crustal thickness of 12 km under the Cape Verde peninsula (Dakar). Burke (1976, fig. 1) reveals the existence of a deep, sediment-filled graben in Senegal (Casamance graben) between 50 and 100 km wide striking for 400 km well within the basin. The development of this graben is associated with the opening of the Atlantic Ocean between 210 and 170 Myr ago. The geology of the graben is poorly known, drilling on one of salt diapirs produced a basement rock of altered basalt (Hayes *et al.* 1971). It is quite likely that the Mesozoic

rifting was widely accompanied by rapid accumulation of several kilometres of sediment and intrusion of magmatic material into fractures (Dillon & Sougy 1974).

Does the MT model support this view? Cenozoic and Mesozoic sediments, with resistivities as low as 1 Ωm may well be associated with saline water in rift fractures. Below the actual post-Jurassic sedimentary basin, the anomalously low resistivity could reflect the presence of fractured wet and possibly altered magmatic material in association with the Ocean opening. The crust in this region was of continental origin, with strong contamination by basaltic intrusions. The measuring site of KOG probably marks the boundary of the Triassic graben in the Precambrian basement and extends over a distance of about 100 km. It is possible that the conductive zone in the upper crust delineates an old zone of weakness which was associated with magmatic activity over a long time during the formation of the Senegal basin. It appears, however, that definite conclusions seem to be still premature or largely speculative. More detailed results may be reached in the future by additional MT soundings, seismic investigations and measurements of the heat flow.

Acknowledgments

Thanks are due to J. Vassal and M. Chauvin for their assistance in this study; especially L. Mollard, the Technical Engineer for the MT equipment since 1972. I am also grateful to P. Perichon and other personnel of the Bondy Laboratory, for computational assistance.

References

Babour, K. & Mosnier, J., 1977. Differential geomagnetic soundings, *Geophysics*, **42**, 66–76.

Babour, K. & Mosnier, J., 1979. Differential geomagnetic soundings in the Rhinegraben, *Geophys. J. R. astr. Soc.*, **58**, 135–144.

Bailey, R. C,, Edwards, R. M., Garland, G. D., Kurtz, R. & Pitcher, D., 1974. Electrical conductivity studies over a tectonically active area in eastern Canada, *J. Geomagn. Geoelect.*, **26**, 125–146.

Banks, R. J. & Ottey, P., 1974. Geomagnetic deep sounding in and around the Kenya rift valley, *Geophys. J. R. astr. Soc.*, **36**, 321–335.

Beblo, M. & Björnsson, A. J., 1978. Magnetotelluric investigation of the lower crust and upper mantle beneath Iceland, *J. Geophys.*, **45**, 1–16.

Berdichevsky, M. N. & Dimitriev, V. I., 1976. Basic principles of interpretation of magnetotelluric sounding curves, in *Geoelectric and Geothermal Studies*, pp. 163–221, ed. Adam, A., Akademiai Kiado, Budapest.

Blohm, E. K., Worzyk, P. & Scriba, H., 1977. Geoelectrical depth soundings in southern Africa using the the Cabora Bassa power line, *J. Geophys.*, **43**, 665–679.

Burke, K., 1976. Development of graben associated with the initial ruptures of the Atlantic Ocean, *Tectonophys.*, **36**, 93–112.

Cantwell, T., 1960. Detection and analysis of low frequency magnetotelluric signals, *PhD thesis*, Massachusetts Institute of Technology.

Compagnie Générale de Géophysique, 1957. *Reconnaissances hydrauliques et structurales par sondages électriques au Sénégal, en Mauritanie et en Casamance*, Paris.

Connerney, J. E. P., Nekut, A. & Kuckes, A. F., 1980. Deep crustal electrical conductivity in the Adirondacks, *J. geophys. Res.*, **85**, 2603–2614.

De Spengler, A. J., Castelain, J. & Leroy, M., 1966. Le bassin secondaire-tertiaire du Sénégal, in *Bassins Sédimentaires du Littoral Africain, Littoral Atlantique*, pp. 80–94, ed. Reyre, D., Symp. Ass. Serv. Géol. Africain, New Delhi, 1964.

Dillon, W. P. & Sougy, M. A., 1974. Geology of West Africa and Canary and Cape Verde Islands, in *The Ocean Basins and Marings, 2. The North Atlantic*, pp. 315–390, eds Nairn, A. E. M. & Stehli, F. G., Plenum Press.

Edwards, R. N., Bailey, R. C. & Garland, G. D., 1981. Conductivity anomalies: lower crust or asthenosphere?, *Phys. Earth planet. Int.*, **25**, 263–272.

Gough, D. I., 1973. The interpretation of magnetometer array studies, *Geophys. J. R. astr. Soc.*, **35**, 83–98.

Gough, D. I., 1981. Magnetometer arrays and geodynamics, in *Evolution of the Earth, Geodynamics Series, Am. geophys. Un.*, **5**, 87–95.

Greenhouse, J. P. & Bailey, R. C., 1981. A review of geomagnetic variation measurements in the eastern United States: implications for continental tectonics, *Can. J. Earth Sci.*, **18**, 1268–1289.

Gregori, G. P. & Lanzerotti, L. J., 1982. Electrical conductivity structure in the lower crust, *Geophys. Surveys*, **4**, 467–499.

Hayes, D. E., Pimm, A. C., Benson, W. E., Berger, W. H., Von Rad, U., Sapko, P. R., Beckmann, J. P., Roth, P. H. & Musich, L. F., 1971. Deep sea drilling project, Leg 14, *Geotimes*, **16**, 14–17.

Hyndman, R. D. & Hyndman, D. W., 1968. Water saturation and high electrical conductivity in the lower continental crust, *Earth planet. Sci. Lett.*, **4**, 427–432.

Ingham, M. R. & Hutton, V. R. S., 1982. The interpretation and tectonic implications of the geoelectric structure of Southern Scotland, *Geophys. J. R. astr. Soc.*, **69**, 595–606.

Jones, A. G. & Hutton, V. R. S., 1979. A multistation magnetotelluric study in Scotland – II. Monte-Carlo inversion of the data and its geophysical and tectonic implications, *Geophys. J. R. astr. Soc.*, **56**, 351–368.

Jupp, D. L. B. & Vozoff, K., 1975. Stable iterative methods for the inversion of geophysical data, *Geophys. J. R. astr. Soc.*, **42**, 957–976.

Kurtz, R. D., 1982. Magnetotelluric interpretation of crustal and mantle structure in the Greenville Province, *Geophys. J. R. astr. Soc.*, **70**, 373–397.

Lebedev, E. B. & Khitarov, N. T., 1964. Dependence of the beginning of melting of granite and the electrical conductivity of its melt on high vapour pressure, *Geochem. Int.*, **1**, 193–197.

Lee, C. D., Vine, F. J. & Ross, R. G., 1973. Electrical conductivity models for the continental crust based on laboratory measurements on high-grade metamorphic rocks, *Geophys. J. R. astr. Soc.*, **72**, 353–371.

Le Pichon, X. & Fox, P. J., 1971. Marginal offsets, fracture zones, and the early opening on the North Atlantic, *J. geophys. Res.*, **76**, 6294–6307.

Liger, J. P., 1980. Structure profonde du bassin côtier sénégalo-mauritanien. Interprétation des données gravimétriques et magnétiques, *Thèse 3ème cycle*, University Aix-Marseille III.

Losecke, W., Knödel, K. & Müller, W., 1979. The conductivity distribution in the North German sedimentary basin derived from widely spaced areal magnetotelluric measurements, *Geophys. J. R. astr. Soc.*, **58**, 169–179.

Madden, T. & Nelson, P., 1964. A defense of Cagniard's magnetotelluric method, *Geophys. lab. O.N.R., Project NR*, pp. 371–401, Massachusetts Institute of Technology.

Mosnier, J. & Yvetot, P., 1972. Nouveau type de variomètre à aimant asservi en direction, *Annls Géophys.*, **28**, 219–224.

Rabinowitz, P. D., 1974. The boundary between oceanic and continental crust in the western North Atlantic, in *The Geology of Continental Margins*, pp. 67–84, eds Burk, C. A. & Drake, C. L., Springer-Verlag.

Ritz, M., 1983. The distribution of electric conductivity on the eastern border of the West African craton (Republic of Niger), *Geophys. J. R. astr. Soc.*, **73**, 475–488.

Schmucker, U., 1970. Anomalies of geomagnetic variations in the south-western United States, *Bull. Scripps Inst. Oceanogr.*, **13**, University of California Press.

Stodt, J. A., 1978. Documentation of a finite element program for solution of geophysical problems governed by the inhomogeneous 2-D scalar Helmholtz equation, *Rep. AER 76-11155, Dept Geol. Geophys.*, University of Utah, Salt Lake City.

Thayer, R. E., 1975. Telluric-magnetotelluric investigations of regional geothermal processes in Iceland, *PhD thesis*, Geological Sciences at Brown University.

Van der Linden, W. J. M., 1981. The crustal structure and evolution of the continental margin off Senegal and the Gambia, from total-intensity magnetic anomalies, *Geologie Mijnb.*, **16**, 257–266.

Van Zijl, J. S. V., 1977. Electrical studies of the deep crust in various provinces of South Africa, in *The Earth's Crust*, ed Heacock, J. G., *Geophys. Monogr. Am. geophys. Un.*, **20**, 470–500, Washington DC.

Vasseur, G., Babour, K., Menvielle, M. & Rossignol, J. C., 1977. The geomagnetic variation anomaly in the northern Pyrénées: study of the temporal variation, *Geophys. J. R. astr. Soc.*, **49**, 593–607.

Vozoff, K., 1972. The magnetotelluric method in the exploration of sedimentary basins, *Geophysics*, **37**, 98–141.